

The anthraquinone derivative Emodin inhibits angiogenesis and metastasis through downregulating Runx2 activity in breast cancer

JUNCHAO MA^{1*}, HONG LU^{2*}, SHAN WANG¹, BIN CHEN¹, ZHAOJIE LIU¹,
XIAOQIN KE¹, TING LIU¹ and JIANJIANG FU¹

¹Department of Pharmacology, College of Pharmacy, ²Modern Education Technology Center, Jiangxi University of Traditional Chinese Medicine, Nanchang 330004, P.R. China

Received October 8, 2014; Accepted December 8, 2014

DOI: 10.3892/ijo.2015.2888

Abstract. Emodin (EMD) is an anthraquinone derivative extracted from the root and rhizome of *Rheum palmatum* L. which exhibits a range of activities, including anti-bacterial, antitumor, diuretic and vasorelaxant effects. The ability to inhibit metastasis and angiogenesis was shown in previous pharmacological studies, but clear information to address EMD affecting angiogenesis and metastasis in human breast cancer is still lacking. In the present study, we evaluated a possible role for EMD in angiogenesis and metastasis induced by breast cancer cells. It was revealed here that EMD attenuated tumor cell-induced metastasis and angiogenesis both *in vitro* and *in vivo*. Furthermore, it was found that these inhibitory effects were caused by MMPs and VEGFR-2 inhibition in metastatic breast cancer cells and endothelial cells, respectively. Western blot analysis showed reduction of Runx2 activation in the EMD-treated cells. ELISA based Runx2 transcription factor assay showed that the interaction between Runx2 and target sequences was inhibited by EMD. Our findings suggested that the inhibitory effects of EMD on tumor-induced metastasis and angiogenesis were caused by MMPs and VEGFR-2 inhibition, which may be associated with the downregulation of Runx2 transcriptional activity.

Introduction

Breast cancer is the most frequent malignant disease and the second cause of death from cancer in US women (1). Most of the patients die of metastases, rather than their primary tumors.

Correspondence to: Dr Jianjiang Fu, Department of Pharmacology, College of Pharmacy, Jiangxi University of Traditional Chinese Medicine, Nanchang 330004, P.R. China
E-mail: jianjiang_fu@yeah.net

*Contributed equally

Key words: Emodin, VEGFR-2, matrix metalloproteinases, Runx2, breast cancer

Although successful treatment of the primary malignancy is achieved as a result of early diagnosis by mammographic screening and implementation of systemic adjuvant therapy (2), relapse and consequent metastatic growth of cancer cells can still occur at distant sites, including bone, lung, liver and brain (3,4). It was reported that metastasis to distant sites accounts for >90% of breast cancer-related mortality (5). However, metastasis remains the most insidious aspect of breast cancer.

How tumors spread and kill their host organism remains an enigma. Over the past decade, research effort on metastatic disease has been focused on the biological processes that influence the establishment of metastases (6,7). It has been well established that tumor metastasis is a complex multistep process that requires migration, invasion and angiogenesis (7). Development of new blood vessels, is a very critical event in formation of metastases. This process is orchestrated by a large number of cytokines and associated receptors and proteinases, such as vascular endothelial growth factor (VEGF), fibroblast growth factor, interleukin-8 and matrix metalloproteinases (MMPs) (8). Breakdown of the extracellular matrix (ECM) is another crucial step in the metastatic cascade. Tumor cells degrade surrounding ECM and basement membrane to facilitate invasion and metastasis by secreting several proteases. MMPs play an important role in this process. It was found that these enzymes participate in proteolysis of ECM, modulation of cell adhesion, migration (9,10), and epithelial to mesenchymal transition (EMT) (11), processing of growth factors, and tumor-induced angiogenesis. Collectively, metastasis comprises multiple consecutive steps, and control one of these processes represent promising therapeutic targets for cancer therapy.

Extensive evidence shows that Runx2 maybe a potential target for inhibition of metastatic growth of breast cancer cells (7). Runx2, also named PEBP2 α A/AMI3/Cbfa1, is a transcription factor which is one of members in runx gene family encoding proteins homologous to *Drosophila* Runt (12). Originally, it is found that this transcription factor plays a crucial role in the formation of the skeleton (13-15). Studies have demonstrated that atypical expression and function of Runx2 are associated with the formation of bone metastasis in breast cancer (16). In addition, Runx2 is ectopically expressed in metastatic cancer

cells but not in non-metastatic cancer cells. Several genes required for bone development and turnover, such as *opn*, *bsp* are major targets of Runx2 (17). Additionally, Runx2 is involved in metastatic foci formation. Accumulating evidence suggests that Runx2 is also a 'master' transcriptional factor in ECs. It is reportedly involved in proliferation (18,19), apoptotic resistance (18), migration and invasion (20) of ECs.

EMD is a natural anthraquinone compound extracted from the root and rhizome of *Rheum palmatum* L. (Fig. 1). This traditional Chinese medicinal herb was widely used for treatment of various ailments and the anti-cancer activity of EMD was demonstrated, and the ability to inhibit metastasis and angiogenesis was also shown (21,22). However, clear information how EMD affects angiogenesis and metastasis in human breast cancer is still required. To further evaluate its potential mechanisms in treatment of metastatic breast cancer, we evaluated the anti-metastatic and anti-angiogenic properties and its underlying mechanisms in this study. We found that EMD inhibited tumor-induced angiogenesis and metastasis *in vitro* and *in vivo*, and that the primary action of EMD in breast cancer cells is through a Runx2-induced inhibitive mechanism.

Materials and methods

Materials. EMD for research use was from Sigma-Aldrich (cat. no. E7881, Beijing, China), with the purity of $\geq 90\%$, as determined by high-performance liquid chromatography. A stock solution (1 mM) was prepared by dissolving EMD in dimethyl sulfoxide (DMSO). Recombinant human VEGF₁₆₅ (cat. no. 293-VE) is a product of R&D Systems (Minneapolis, MN, USA). A potent inhibitor of VEGFR-2, ZD6474 (Selleck Chemicals Inc., cat. no. S1046, Shanghai, China), and a broad spectrum MMP inhibitor, Batimastat (Bat; Santa Cruz Biotechnology Inc., cat. no. SC-203833, Santa Cruz, CA, USA) were used in this study and served as positive controls. In addition, L-sulforaphane (SFP, Sigma-Aldrich, cat. no. S6317, Beijing, China) was used as a positive control in tube formation assay.

Cell culture. The human umbilical vein cell line, EA.hy 926, was purchased from cell bank of Shanghai Institute for Biological Sciences, CAS. EA.hy 926 cells were maintained in Dulbecco's modified Eagle's medium supplemented with 10% FBS, 100 IU/ml penicillin and 100 μ g/ml streptomycin (Invitrogen, Beijing, China) in a humidified incubator containing 5% CO₂ at 37°C. Prior to performing each assay, the ECs were serum starved for 4 h. MDA-MB-231 human breast cancer cells, purchased from Cell Resource Center, Institute of Basic Medical Sciences, Chinese Academy of Medical Sciences, were maintained in Dulbecco's modified Eagle's medium (DMEM) supplemented with 10% fetal bovine serum (FBS; Gibco, Inc.), 100 IU/ml penicillin and 100 μ g/ml streptomycin (Invitrogen, Inc.) in a humidified incubator containing 5% CO₂ at 37°C.

Animals and ethics statement. Five- to-six-week-old female NOD/SCID mice were purchased from Vital River Laboratories (Beijing, China) to establish orthotopic and experimental lung metastatic xenograft model. Eight- to-nine-week-old male Sprague Dawley (SD) rats were also purchased from Vital

River Laboratories to obtain thoracic aorta in the rat aortic ring angiogenesis assay. The animal experimental protocol complied with the Animal Management Rules of the Chinese Ministry of Health (document no. 55, 2001), and was approved by the Animal Ethics Committees of Jiangxi University of Traditional Chinese Medicine. All of the animal experiments were conducted in strict accordance with the requirements listed in this protocol. All surgery was performed under sodium pentobarbital anesthesia, and all efforts were made to minimize suffering.

In vivo growth assay. For the growth assay, MDA-MB-231 cell xenografts were established by injection of 1×10^7 cells at the mammary fat pad in NOD/SCID mice. After 3 weeks of growth, the tumors were removed and $1 \times 1 \times 1$ mm tumor pieces were then implanted at the mammary fat pad of mice. The mice bearing tumor chunks were randomly divided into three groups: control, EMD (40 mg/kg per day) treatment group, and EMD (80 mg/kg per day) treatment group. Forty-eight hours later, EMD was administered by gavage on a regimen of 6-day dosing per week for 5 weeks. Tumor growth was assessed by measuring volumes of tumors with electronic calipers every 3-4 days continuously. All of the mice were sacrificed 5 weeks after inoculation of the cancer cells and the tumors were collected and weighed.

In vivo experimental metastasis assay and survival assay. To establish experimental lung metastasis xenograft model, 2×10^6 MDA-MB-231 cells in 200 μ l normal saline were injected through tail vein of NOD/SCID mice. The mice were divided into control, EMD (40 mg/kg per day) treatment group, and EMD (80 mg/kg per day) treatment group. EMD treatment was began 24 h after tumor injection. After 8-week treatment the formation of metastatic foci in lung tissues was measured by nest reverse-transcription polymerase chain reaction (RT-PCR). The mice were euthanized and dissected, and lungs were snap frozen in liquid nitrogen. Total RNA was isolated from each lung using the QIAshredder and RNeasy Protect Mini kit (Qiagen) for detection of human cytokeratin 19 (ck19) by nest PCR. For the survival assay, the experimental lung metastasis xenograft model was established using the same method as *in vivo* experimental metastasis assay, but the observation period was 120 days.

RNA isolation and nest RT-PCR. Nest RT-PCR was used to detect expression of the human ck19 gene in lung tissues of tumor-bearing mice. Total RNA was isolated from each lung using the QIAshredder and RNeasy Protect Mini kit (Qiagen). Ck19 was reverse transcribed in the presence of 2 μ l enzyme mix, 10 μ l RNA and outer primer for 30 min at 50°C, according to the manufacturer's instructions (Qiagen OneStep RT-PCR kit, Qiagen). After Taq polymerase activation for 15 min at 95°C, samples were amplified for 37 cycles at 94°C for 45 sec, 58°C for 45 sec and 72°C for 90 sec. Target primers for amplifying ck19 (outer primer) were designed using Primer Designer (Scientific & Educational Software Version 2.0). The forward primer for ck19 (GenBank no. BC010409) was 5'-cca cgt cgt cct tcg gag gcc-3' (64-84 bp) and reverse primer was 5'-gttc cgt ctc aaa ctt ggt tc-3' (529-549 bp). After a final extension for 10 min at 72°C, the RT-PCR product was

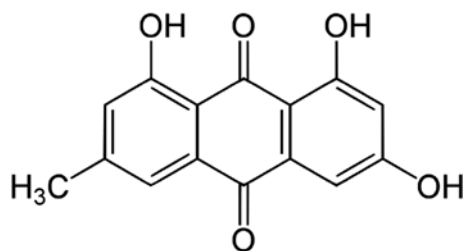


Figure 1. Molecular structure of Emodin.

further subjected to nest PCR using the Qiagen Multiplex PCR kit (Qiagen). The inner primers were forward 5'-tac agc cac tac tac acg acc atc c-3' (432-456 bp) and reverse 5'-gga caa tcc tgg agt tct caa tg-3' (488-510 bp). The nest PCR profile was as follows: 3 min at 94°C, followed by 35 three-step cycles of 45 sec at 94°C, 45 sec at 60°C and 1 min at 72°C. PCR reactions were subjected to final extension at 72°C for 10 min. Nest RT-PCR analysis was performed using the Mastercycler gradient (Eppendorf). The β -actin gene was used as an internal control for standardization and the primers, Tm, and cycles are the same as reported (23). The nest PCR product was separated by 4% agarose (UltraPure™ Agarose, Invitrogen) gel electrophoresis, and the gels were viewed by UV transillumination and photographed by the UVP EC3 gel imaging system.

Immunohistochemistry for tumor tissues. MVD was determined by CD34 staining against ECs in tumor tissues. Firstly, 4- μ m-thick sections from paraffin-embedded formalin-fixed MDA-MB-231 tumor tissues were made. After dewaxing, and hydration, the slides were incubated with Proteinase K at 37°C for 15 min to retrieve antigen, and then washed in PBS (0.01 mol/l, 5 min, three times). In order to block endogenous peroxidase activity, the sections were treated with 3% H₂O₂ in methanol for 10 min. Followed by blocking with 10% normal goat serum (Cell Signaling, Danvers, MA, USA) and washing in PBS, the slides were incubated with anti-CD34 antibody (1:50; cat. no. 3569; Cell Signaling) or PBS (0.01 mol/l) at 4°C overnight. The slices were incubated with second antibody (HRP-labeled goat anti-mouse antibody) at room temperature for 60 min, and then peroxidase activity was detected by SignalStain® DAB substrate kit (Cell Signaling). All the slides were checked under light microscopy (Olympus, BX-63), and images were analyzed by Image Pro plus software 5.0 (Media Cybernetics Inc. Silver Spring, MD, USA).

Tube formation assay. The tube formation assay was used to investigate the effects of EMD on angiogenesis *in vitro*. Briefly, 80 μ l of liquid growth factor-reduced Matrigel (BD Biosciences, San Jose, CA, USA) were added to each well of a 96-well plate. After 45-min incubation at 37°C, 3x10⁴ EA.hy 926 cells per well in 100 μ l complete culture medium containing vehicle, ZD6474 or EMD was seeded in each well. Then, 100 μ l serum-free medium containing VEGF₁₆₅ (final concentration 2 ng/ml) was added. After 24-h incubation at 37°C and 5% CO₂, the images of each well were recorded by an inverted microscope (Leica, DMI 3000B, Germany).

Rat aortic ring angiogenesis assay. In the present study, an *ex vivo* tube formation system was used to evaluate the anti-angiogenic effect of EMD. Male SD rats (8-9-week-old) were euthanized and thoracic aortas were retrieved. After rinsing with 1% antibiotic/antimycotic cocktail in 1X PBS (100 U/ml penicillin, 100 μ g/ml streptomycin and 0.25 μ g/ml amphotericin B; Invitrogen), the surrounding fibro-adipose tissue of thoracic aorta was completely removed with fine microdissection scissors and the thoracic aorta was cut into 1 mm thick rings with a scalpel blade. Then, individual ring was implanted on a Matrigel-coated 96-well microtiter plate. Matrigel was added again to embed and fix rings. After 30-min incubation in 5% CO₂ at 37°C, the aorta rings were incubated in human endothelial serum-free medium (Gibco, Carlsbad, CA, USA) supplemented with 2% FBS, 50 U/ml penicillin and 50 μ g/ml streptomycin (Invitrogen) for 24 h and then treated with different doses of EMD for 13 days. Finally, 8 μ g/ml Calcein AM (BD Biosciences) was added to stain microvessels. Photographs of the microvessels were obtained using an inverted fluorescence microscope (Leica, DMI 3000B, Germany).

In vitro invasion assay. Effects of EMD on invasion were measured by a 48-well microchemotaxis system (AP 48, Neuro Probe; Gaithersburg, MD, USA). Briefly, 5 μ g of fibronectin in a volume of 50 μ l was applied on the rough (lower) surface of the polycarbonate membrane and 5 μ g/filter Matrigel was plated to the smooth (upper) surface. The lower chambers of the plates were then filled with 30 μ l medium containing 0.1% BSA. Log-phase cells were harvested and re-suspended in culture medium with 0.1% BSA. Cell suspensions (100 μ l containing 1x10⁵ cells) were added to the upper compartment and incubated for 16 h at 37°C in a 5% CO₂ atmosphere. After incubation, the filters were fixed with methanol and stained with 0.5% crystal violet for 60 min. The cells on the upper surface of the filters were removed by wiping with cotton swabs. The cells invading to the lower surface of the filter through Matrigel and filter were quantified with the Image Pro plus software 5.0 (Media Cybernetics Inc.), and representative results are illustrated in the figures. Each assay was performed in triplicate.

In vitro migratory assay. *In vitro* migration of MDA-MB-231 cells was measured using the AP 48 chamber (Neuro Probe), similar to the *in vitro* invasive assay, but without Matrigel pre-coating on the smooth (upper) surface of filters. Briefly, the underside of the polycarbonate membrane was coated with 10 μ g/ml fibronectin overnight at 4°C. Thirty microliters of DMEM (with 10% FBS and 10 μ g/ml Collagen I) was added to the lower chamber, and the chamber was covered by the filter. MDA-MB-231 cells were trypsinized and washed with FBS-free DMEM, and 100 μ l of cell suspensions (in FBS-free DMEM, containing 2x10⁵ cells) with or without EMD were added to the upper chambers and incubated for 14 h in an incubator containing 5% CO₂ at 37°C. Determination of migrated cells was conducted as described for the *in vitro* invasive assay.

Immunocytochemistry. Log-phase cells EA.hy 926 cells were harvested, re-suspended and seeded on the 8 wells Nunc™ Lab-Tek™ II Chamber Slide™ system. The cells were grown

at 37°C in a humidified CO₂ incubator until they were 50-70% confluent. The culture medium was aspirated from each well and the cells gently rinse twice in PBS at room temperature. Then, the cells were exposed to EMD and/or vehicle for 24 h. After exposure, the chambers of the Chamber Slide system were removed gently and the slides were rinsed twice in PBS. Then cells were fixed by incubation in 4% (v/v) paraformaldehyde in PBS for 20 min at room temperature. The slides were heated in antigen retrieval buffer [100 mM Tris, 5% (w/v) urea, pH 9.5] at 95°C for 10 min. After rinsed in PBS, cells were blocked by incubating the cells in 0.1% Triton X-100 in PBS for 15 min at room temperature. Then, cells were incubated with the primary antibodies at 4°C overnight. After rinsing in PBS, the slices were incubated with second antibody (HRP-labeled goat anti-mouse antibody) at room temperature for 60 min, and then peroxidase activity was detected by SignalStain[®] DAB substrate kit (Cell Signaling). All the slides were checked under a light microscope (Olympus, BX-63), and images were analyzed by Image Pro plus software 5.0 (Media Cybernetics Inc.).

FRET-based MMP activity assay. The activity of MMPs was measured by the SensoLyte[®] 570 Generic MMP assay kit (AnaSpec, Fremont, CA, USA). This kit provides a FRET-based method to detect the activity of a variety of MMPs including MMP-1, 2, 3, 7, 8, 9, 10, 11, 12, 13 and 14. It uses 5-FAM (fluorophore) and QXL520[™] (quencher) labeled FRET peptide substrates for continuous measurement of MMP activity. In an intact FRET peptide, the fluorescence of 5-FAM is quenched by SensoLyte. Upon the cleavage of FRET peptide by MMPs, the fluorescence of 5-FAM is recovered. Analyses were performed according to the manufacturer's instructions. Briefly, supernatants of MDA-MB-231 cells were collected after incubation with or without EMD for 12 h. MMPs in the supernatants were activated by incubation with 4-aminophenylmercuric acetate for 1 h at 37°C. Fifty microliter MMPs-containing samples and 50 μ l MMP substrate solution were added into a 96-well plate. The reagents were mixed by shaking the plate gently for 30 sec. After a 50-min incubation period at 37°C, the counter Victor3[™], Perkin-Elmer (Waltham, MA, USA) was applied at Ex/Em=540 nm/575 and then the action was stopped by adding stop solution, and fluorescence intensity was measured.

Runx2 transcription factor assay. Runx2 activity in MDA-MB-231 and EA.hy 926 nuclear extracts was detected using the TransAM[™] AM1-3/Runx2 kit (Active Motif North America, Carlsbad, CA, USA) following the manufacturer's instructions. Cell extracts were prepared using the nuclear extract kit (Active Motif). Then, 20 μ l of extracts diluted in complete lysis buffer and containing 15 μ g nuclear extract were added into a 96-well plate. This plate immobilizes oligonucleotides containing Runx2 consensus binding sites. Saos-2 nuclear extract served as a positive control for Runx2 activation and 20 μ l complete lysis buffer served as the blank. The wild-type consensus oligonucleotide was provided as a competitor for Runx2 binding to monitor the specificity of the assay. After 1-h incubation at room temperature, the plate was washed three times with washing buffer. Diluted primary antibody (100 μ l) was added into wells and incubated for 1 h

at room temperature without agitation. After three washes, HRP-labeled secondary antibody was added and incubated for 1 h at room temperature. Then, 100 μ l developing solution was added to initiate the color reaction. After 100 μ l stop solution was added, the absorbance was measured within 5 min at 450 nm with a reference wavelength of 655 nm using an ELx800 microplate reader (BioTek, Winooski, VT, USA).

Western blot analysis. For western blot analysis, ECs were washed twice with PBS and then lysed by the addition of 1 ml lysis buffer (10 mmol/l Tris, pH 7.6, 150 mmol/l NaCl, 5 mmol/l EDTA, pH 8.0, 10 ml/l Triton X-100, 1 mmol/l DTT) containing 0.1 mmol/l PMSF. After 30 min on ice, lysates were collected and clarified by centrifugation at 15,000 g for 10 min at 4°C. Aliquots of whole cell lysates were subjected to 10% SDS-PAGE and then transferred to Hybond nitro-blotting membranes. The membranes were blocked with 3% bovine serum albumin in Tris-buffered saline containing 0.5 ml/l Tween-20 (TTBS) and then incubated with a 1:500-1,000 dilution of the indicated primary antibodies, followed by incubation with horseradish peroxidase (HRP)-conjugated secondary antibodies. Immunoreactive proteins were detected using an enhanced chemiluminescence kit (Millipore). β -actin (Santa Cruz, SC-130301) served as an internal control.

Statistical analysis. The mean values were obtained from at least three independent tests. The data are presented as mean \pm SD and analyzed with the GraphPad Prism 5.0 software program (La Jolla, CA, USA). Comparison among different groups was carried out by analysis of variance (one-way ANOVA). Differences between means were considered statistically significant at $p < 0.05$.

Results

EMD inhibits tumor growth and development of metastasis *in vivo*. Initially the study was to determine the inhibitory effects of EMD on breast cancer *in vivo*. The growth inhibition in MDA-MB-231 cell line-xenografts was determined first. Tumor-bearing mice were treated with various doses of EMD for 5 weeks. A significant suppression on tumor weight was found when the mice were treated with 80 mg/kg b.w. of EMD (Fig. 2A). These results indicated that EMD may contribute to breast cancer. Considering the clinical importance of metastasis in breast cancer patients, the role of EMD in inhibition of metastasis was evaluated *in vivo*. Experimental lung metastasis models were established by injecting human breast cancer MDA-MB-231 cells through tail vein of NOD/SCID mice and the tumor cells invaded into lung tissues were detected by amplification of human ck19 gene with nest RT-PCR assay. As shown in Fig. 2B, EMD at 80 mg/kg b.w. daily for 8 weeks reduced >70% ck19 expression compared to the vehicle control. To determine whether EMD influence survival of the tumor cell injected mice, overall survival assay was performed. Our data showed that EMD lengthen survival time of NOD/SCID mice in a dose-dependent manner (Fig. 2C).

EMD inhibits invasion and migration of MDA-MB-231 cells *in vitro*. Invasion and migration are the critical steps for the

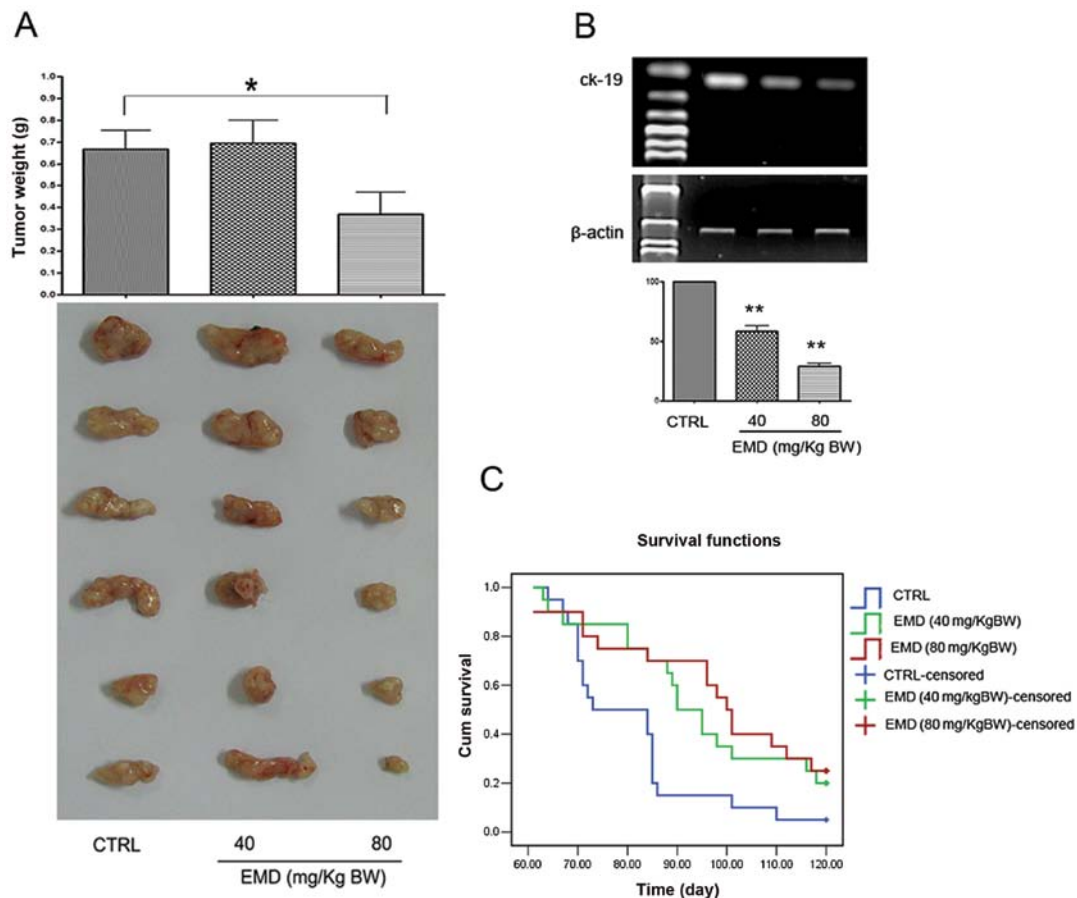


Figure 2. The anti-tumor properties of EMD. EMD inhibited tumor growth of MDA-MB-231 cells *in vivo* (A). EMD induced a significant inhibitory effect on the formation of lung metastatic foci (B) and a considerable increase of overall survival (C) in NOD/SCID mice. Orthotopic and experimental lung metastasis xenograft models were established according to Materials and methods. Lung metastatic foci were determined by nested RT-PCR. Total RNA was extracted from each lung tissue. RNA extracted from the CTRL group served as CTRL. * $p < 0.05$; ** $p < 0.01$ compared with CTRL. EMD, Emodin; CTRL, control.

spread of tumor cells to distant organs. To determine whether inhibition of lung tumor formation by EMD *in vivo* was due to the ability of EMD to influence tumor cell migration and/or invasion, we next determined the effects of EMD on cell invasion and migration *in vitro*. As shown in Fig. 3A, EMD blocked trans-membrane invasion of MDA-MB-231 cells significantly, when MDA-MB-231 cells were incubated with 10, 20 and 40 μM EMD for 14 h. We next evaluated the effects of EMD on cell migration with similar methods. Here, we also found that migration of MDA-MB-231 cells was significantly blocked by EMD (Fig. 3B) in a dose-dependent manner. The data suggested that the inhibitory effects of EMD on metastasis may be associated with its significant inhibition on cell invasion and migration.

EMD inhibits the activity of MMPs in MDA-MB-231 cells *in vitro*. Breakdown of the extracellular matrix by MMPs in surrounding tissues is a fundamental step of invasion and migration in tumor cell metastasis. Therefore, we examined the effects of EMD on MMPs in MDA-MB-231 cells. Fig. 4 shows the effects of EMD on MMPs in MDA-MB-231 cells. Using a fluorescence resonance energy transfer (FRET)-based analysis, we found that EMD exhibited significant suppression of FRET substrate cleavage of MMPs in a dose-dependent manner (Fig. 4A). To further determine whether EMD inhibited the functional activity or expression of MMPs, we analyzed the

expression of MMP-9 and MMP-13 in MDA-MB-231 cells treated with EMD. As shown in Fig. 4B, EMD significantly decreased MMP-9 and MMP-13 expression of MDA-MB-231 in a dose-dependent manner. These data suggested that the anti-metastatic properties of EMD may be due to downregulation of expression of MMP-9 and MMP-13 in MDA-MB-231 cells.

EMD inhibits the development of angiogenesis *in vivo*. To determine whether tumor growth and metastasis inhibition by EMD was associated with inhibition of tumor vessel formation, we next measured effects of EMD on microvessel density (MVD) in MDA-MB-231 tumor blocks by IHC assay. Representative results are illustrated in Fig. 5 and semi-quantitative analysis of CD34 in these tumor blocks was shown in Table I. A 42.49% ($p < 0.01$ compared with CTRL) and 78.91% ($p < 0.01$ compared with CTRL) reduction of positive area of CD34 staining were observed when the nude mice were treated with 40 and 80 mg/kg/day EMD, respectively.

EMD shows direct inhibitory effects on angiogenesis by targeting endothelial cell activation. To determine whether inhibition of tumor induced angiogenesis *in vivo* by EMD was due to a direct inhibition targeting ECs, we used the tube formation assay to evaluate the effects of EMD on angiogenesis. As shown in Fig. 6A, when EA.hy 926 cells were seeded on Matrigel, capillary-like structures with a lumen

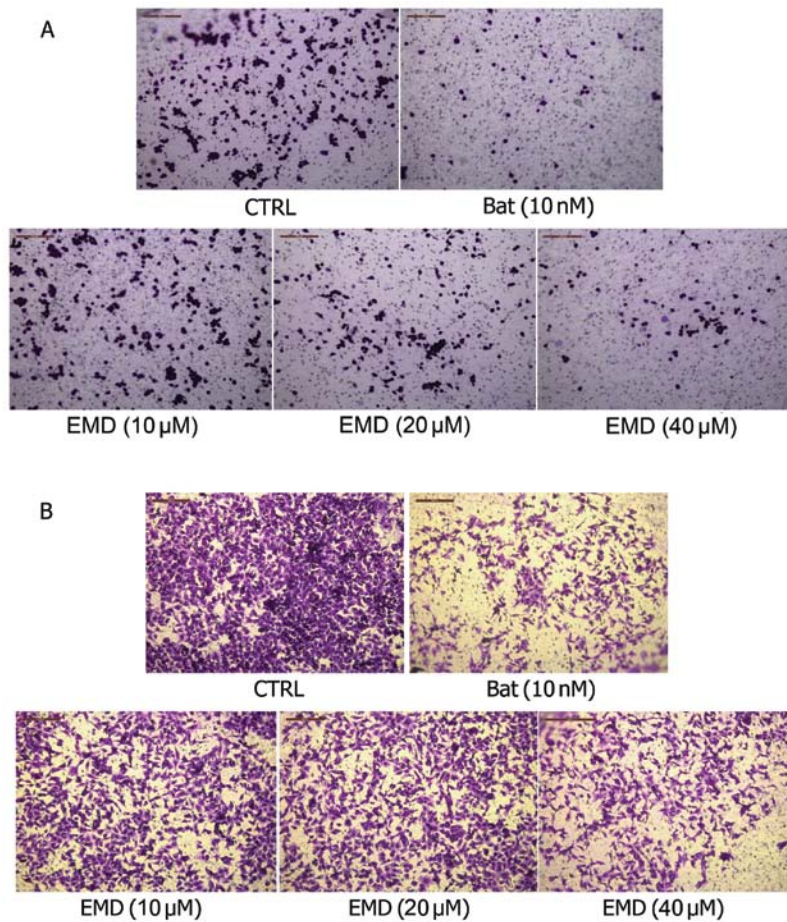


Figure 3. Effects of EMD on *in vitro* invasion and migration of MDA-MB-231 cells. (A) EMD inhibited the invasion of MDA-MB-231 cells in the AP48 chamber. Five fields were counted for each chamber and each concentration was repeated in three chambers. (B) Effects of EMD on migration of MDA-MB-231 cells. *In vitro* invasion and migration assay were carried out as described in Materials and methods. Vehicle (DMSO) was used as a CTRL and Bat served as the positive CTRL. Each assay was performed in triplicate. EMD, Emodin; CTRL, control; Bat, Batimastat.

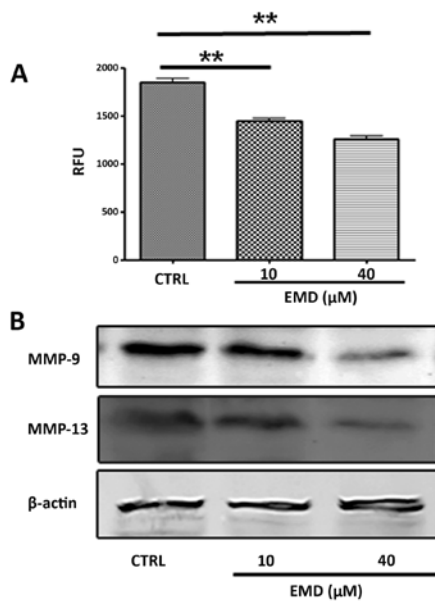


Figure 4. Effects of EMD on activity of matrix metalloproteinases in MDA-MB-231 cells. (A) MMP protein activity was detected by the FRET-based MMP activity assay kit. (B) EMD inhibited MMP-9 and MMP-13 expression in MDA-MB-231 cells as detected by western blotting. Vehicle (DMSO) was used as a CTRL. ***p*<0.01 compared with DMSO-treated cells. Each assay was performed at least in triplicate. All MDA-MB-231 cells were treated with EMD for 18 h. EMD, Emodin; CTRL, control.

Table I. Semi-quantitative analysis of CD34 in MDA-MB-231 tumor tissues.

Group	Relative area of CD34 immunostaining (%)	Inhibition rate (%)
Negative	0.87±0.22	-
CTRL	10.05±2.47	-
EMD 40 mg/kg/day	5.78±2.23 ^a	42.49
EMD 80 mg/kg/day	2.12±0.81 ^a	78.91

^a*p*<0.01 compared with CTRL. EMD, Emodin; CTRL, control.

were formed. After exposure to EMD solution at various concentrations for 24 h, these structures were destroyed in a dose-dependent manner. In addition, rat aortic ring angiogenesis assay was used in this study to verify the anti-angiogenic effects of EMD. Similarly, new blood vessels, triggered by the injury of the dissection procedure and mediated by growth factors produced from aortic ring were demolished by EMD in a dose-dependent manner (Fig. 6B).

EMD inhibits VRGFR-2 activation of endothelial cells in vitro. VEGFR-2 is a crucial regulator in all aspects of normal and

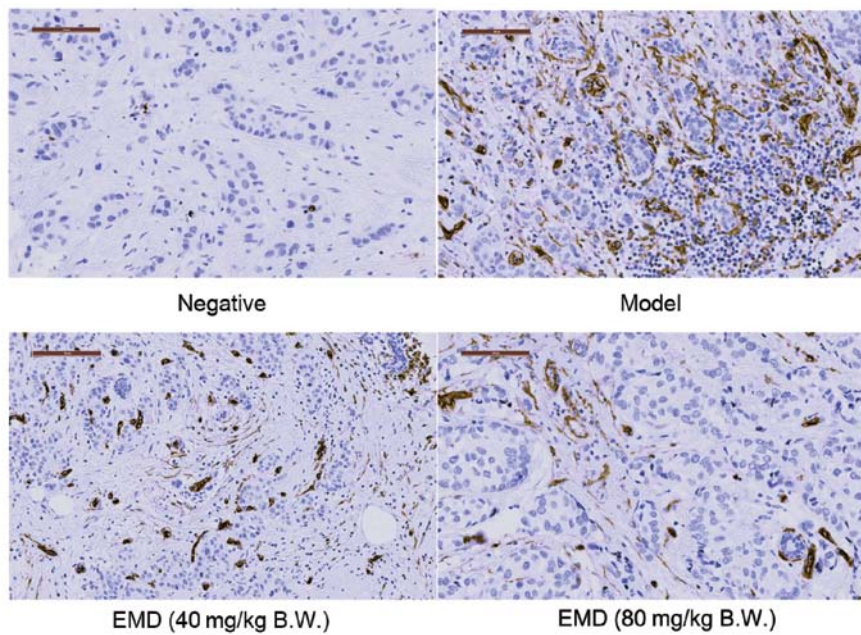


Figure 5. Effects of EMD on tumor-induced angiogenesis in human breast cancer. The expression of CD34 was determined by immunohistochemical assay in MDA-MB-231 tumor tissues. Slides of no primary antibody served as negative control, and the mice treated with normal saline.

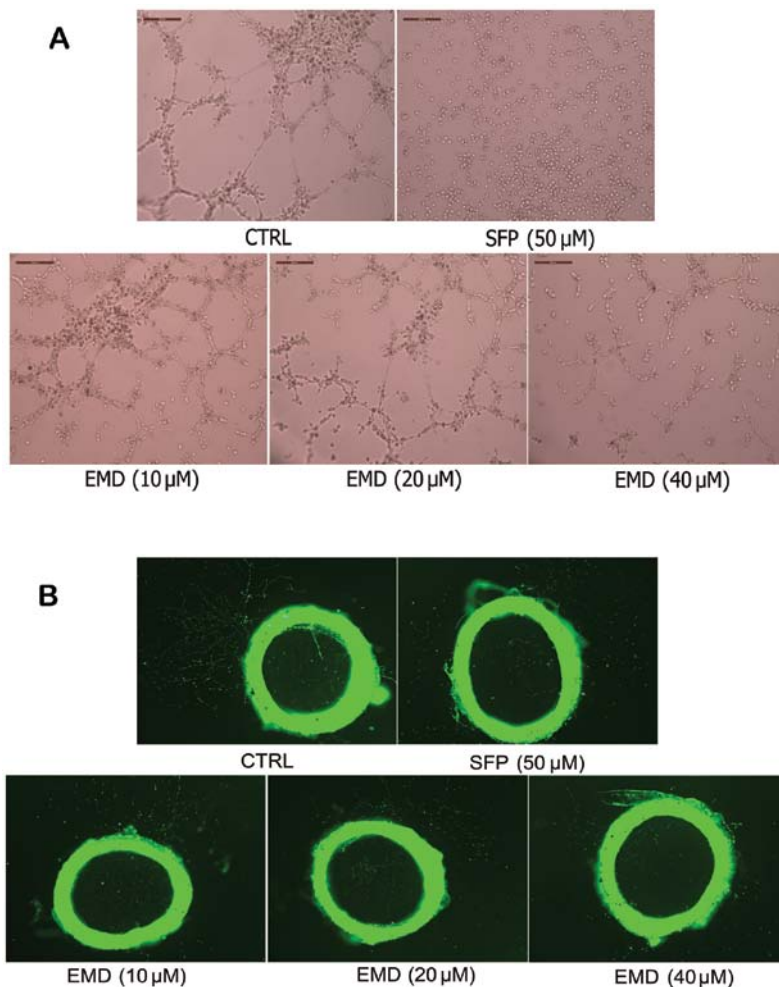


Figure 6. Effects of EMD on *in vitro* and *ex vivo* tube formation of ECs. (A) EMD inhibited mesh-like structure formation of EA.hy 926 cells on Matrigel when the cells were exposed to EMD for 24 h. (B) EMD showed an overt suppression of tube formation *ex vivo* evaluated by rat aortic ring angiogenesis assay. Rat aortic ring angiogenesis assay was performed according to Materials and methods. Five fields were counted for each well, and each concentration was repeated in three wells. Vehicle (DMSO) was used as a CTRL, and SFP served as the positive control. All treatments were conducted in presence of 2 ng/ml VEGF₁₆₅. EMD, Emodin; CTRL, control; SFP, L-sulforaphane.

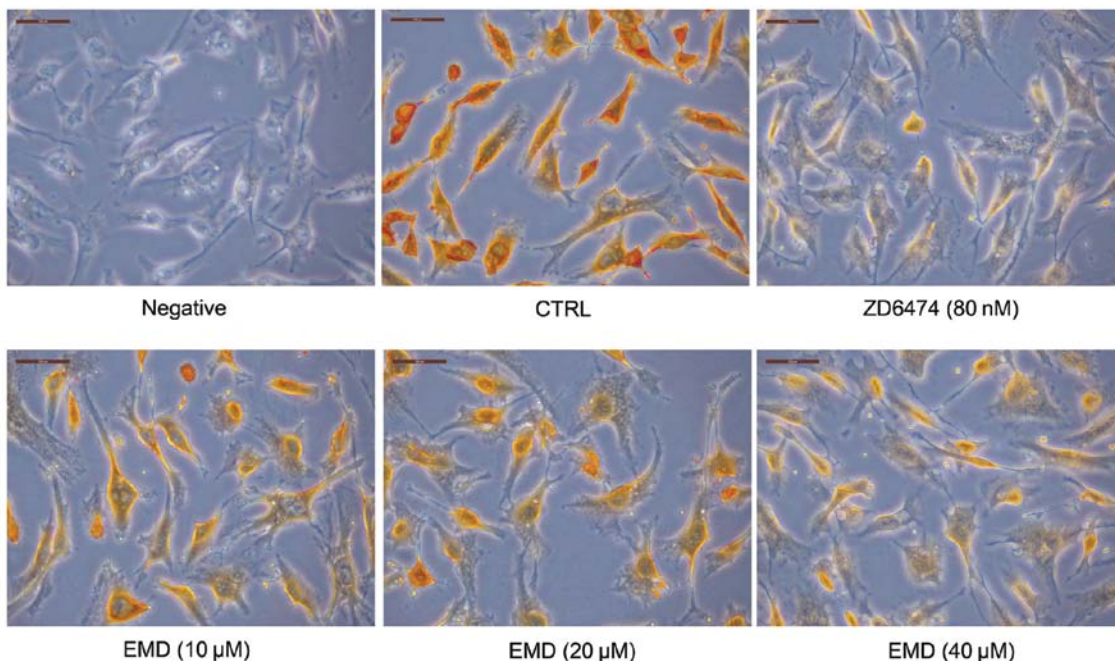


Figure 7. Effects of EMD on activation of VEGFR-2 in endothelial cells. The expression of phospho-VEGFR-2 was determined by immunocytochemistry assay in EA.hy 926 cells. Slides of no primary antibody served as negative control. ZD6474 served as positive control. All ECs were treated with EMD for 24 h in presence of 2 ng/ml VEGF₁₆₅. EMD, Emodin; CTRL, control.

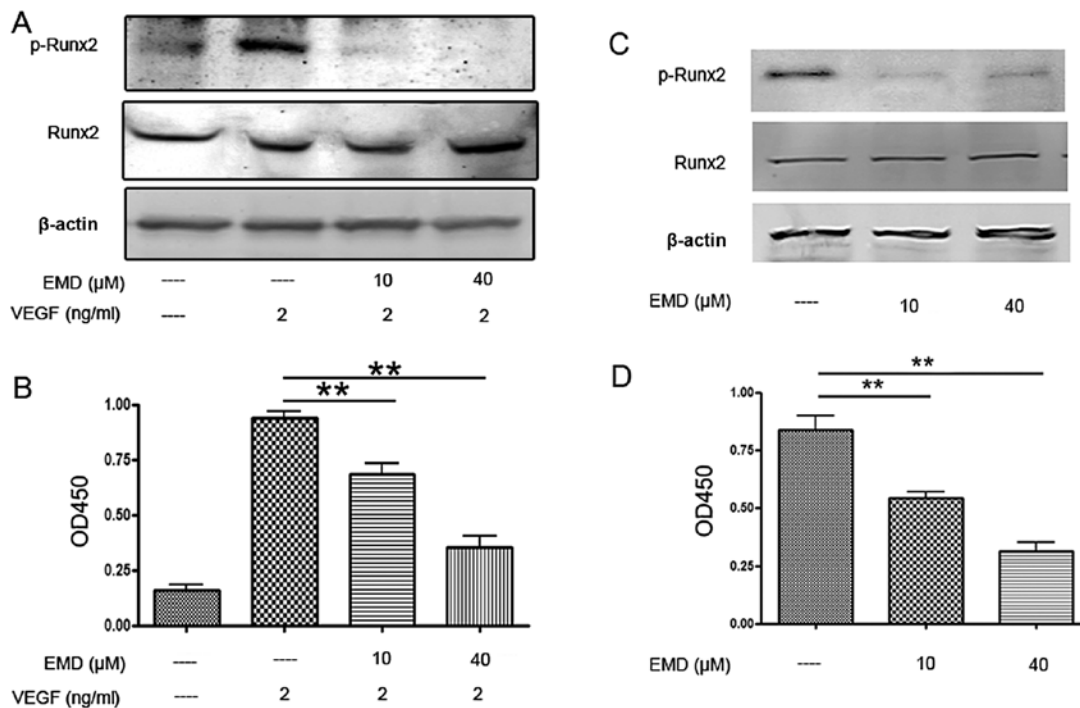


Figure 8. Effects of EMD on Runx2 in MDA-MB-231 and EA.hy 926 cells. EMD suppressed phosphorylation and transcription factor activity of Runx2 as detected by western blotting (A) and Runx2 transcription factor assay kit (B) in EA.hy 926 cells and in MDA-MB-231 cells (C and D). Vehicle (DMSO) was used as a CTRL. All the cells were exposed to EMD for 18 h. **p<0.01 compared with CTRL. EMD, Emodin; CTRL, control.

pathological vascular endothelial cell biology. In order to understand whether VEGFR-2 is involved in the inhibition of angiogenesis induced by EMD, we next evaluated the effects of EMD on VEGFR-2 phosphorylation in EA.hy 926 cells. To this end, immunocytochemistry assay was employed and the results are shown in Fig. 7. From these data, it was found that EMD produced a dose-dependent decrease in phospho-

VEGFR-2 expression. Collectively, these findings indicated that EMD inhibited angiogenesis by directly inhibiting activation of VEGFR-2 in human ECs.

EMD inhibits activation of Runx2 in endothelial and MDA-MB-231 cells. Runx2 is a transcriptional factor of metastatic growth of breast cancer cells. Several genes required for

the formation of metastatic foci, including MMP-9, MMP-13, bone sialoprotein, osteopontin, VEGF, are targets of this transcriptional factor. Therefore, next we examined Runx2 activities in ECs and MDA-MB-231 cells. As shown in Fig. 8A and C, EMD had no effect on total Runx2 expression, but caused a significant decrease of phospho-Runx2 expression. To confirm the western blot results, Runx2 transcription factor assay was employed. Here, an ELISA-based kit for the Runx2 transcription factor was used to analyze the effects of EMD on Runx2. Nuclear extracts incubated with EMD or vehicle were prepared and the binding activity between Runx2 with its target sequence was determined. The results showed that EMD significantly decreased the binding activity of Runx2 to its target sequences in EA.hy 926 and MDA-MB-231 cells (Fig. 8B and D). Together, these findings suggested that the inhibitory effects of EMD on angiogenesis and metastasis were caused by inhibition of MMPs and VEGFR-2, which may be associated with suppression of Runx2 phosphorylation.

Discussion

Emodin is an anthraquinone derivative of the root and rhizome of *Rheum palmatum* L. and also found in other plants (24). This active compound has been reported to show anti-bacterial, antitumor, diuretic and vasorelaxant effects (24). EMD reportedly inhibits tumor-induced angiogenesis and metastasis by blocking VEGFR signaling in human colon cancer cells and inhibiting MMP expression in human neuroblastoma cells (25). However, there is no clear information how EMD affects angiogenesis and metastasis in human breast cancer. Therefore, we evaluated the inhibitory effects of EMD on angiogenesis and metastasis in breast cancer. We found that this anthraquinone derivative showed significant antitumor properties and improvement of overall survival in human breast cancer. It was found that EMD attenuated tumor cell-induced angiogenesis and metastasis both *in vitro* and *in vivo*. Furthermore, these inhibitory effects of EMD were caused by MMPs and VEGFR-2 inhibition, which may be associated with downregulation of Runx2 transcriptional activity in breast cancer.

Migration and invasion of tumor cells are critical events in the metastatic processes. In addition, breakdown of the extracellular matrix by MMPs in surrounding tissues is a fundamental step of invasion and migration in tumor cell metastasis. Thus, in the present study, we examined the anti-metastatic properties of EMD *in vitro* and *in vivo*. It was demonstrated that EMD decreased tumor foci formation in experimental metastasis *in vivo* and inhibited tumor cells invasion and migration *in vitro*. FRET-based MMPs analysis and western blot assay indicated that EMD attenuated MMP activity and expression of MMP-9 and MMP-13. MMPs are a family of structurally and functionally related zinc-dependent endopeptidases. To date, 23 human MMPs, including 17 soluble, secreted enzymes and six membrane-associated enzymes, have been identified (10). These enzymes are involved in a wide range of physiological and pathological processes, such as embryonic development, wound healing, tumor growth, invasion and metastasis (9), and participate in the proteolysis of the ECM, modulation of cell adhesion, migration, and EMT, processing of growth factors, and tumor-

induced angiogenesis. In breast cancer, reported data suggested critical roles for MMPs in both breast cancer initiation and progression (9,11,26). These data suggested EMD attenuation of breast cancer metastatic properties may be associated with inhibition of MMPs.

It is well recognized that the growth of both primary and metastatic tumors depends on adequate vascular support. The increase in vasculature also increases the ability of tumor cells to invade, enter the circulation to reach distant organs and give rise to metastasis (27). In order to understand the anti-growth and anti-metastatic properties of EMD in breast cancer, we also evaluated its anti-angiogenic effects. Our data showed that EMD inhibited the development of angiogenesis in MDA-MB-231 breast cancer. Then, we used tube formation assay of ECs and rat aortic ring angiogenesis assay to evaluate the anti-angiogenic effects of EMD. It was revealed that mesh-like structure formation on Matrigel was significantly impaired by EMD both in tube formation assay and in rat aortic ring angiogenesis assay, when 2 ng/ml of VEGF was added into the culture system. Because of the important role of VEGFR signaling in tumor-induced angiogenesis, we next determined the activity of VEGFR-2 in ECs. Immunocytochemistry assay indicated that EMD suppressed expression of phospho-VEGFR-2 in EA.hy 926 cells significantly. These data suggested that the direct effects of EMD on ECs may also contribute its inhibitory properties on tumor growth and metastasis.

Runx2, also named PEBP2 α A/AM13/Cbfa1, is a critical transcription factor for osteoblastic differentiation and skeletal morphogenesis. This protein belongs to the Runx family encoding proteins homologous to *Drosophila* Runt and has a conserved Runt DNA-binding domain. Originally, Runx2 was found to act as a master regulatory factor in skeletal development (15). To date, extensive evidence shows a close association between Runx2 and breast cancer metastasis, and this transcriptional factor is becoming a potential target of novel antimetastatic agents and diagnostic approaches to breast cancer control (28-30). Jiménez *et al* first found that MMP-13, also named Collagenase-3, was highly expressed in MDA-MB-231 cells, and that it was one of target genes of Runx2 (31). These observations were demonstrated by Selvamurugan and colleagues (32,33). Studies showed that the runt domain (RD) binding site and Runx2 were required for maximal constitutive and basal expression of MMP-13 in MDA-MB-231 cells. ChIP assay confirmed two Runx2 binding sites in the MMP-13 promoter, and these sites are occupied by Runx2. Pratap *et al* investigated the role of Runx2 in the regulation of the promoter of MMP-9, in MDA-MB-231 and MCF-7 cells (34). Collectively, Runx2 acts a 'master' transcription factor of MMPs expression. Therefore, we wondered whether the inhibitory effects of EMD on MMP-9 and MMP-13 were associated with the downregulation of Runx2 activities in breast cancer cells. Our findings from western blotting demonstrated that EMD significantly inhibited the expression of p-Runx2 indicating that the transcriptional ability of Runx2 is impaired by EMD. To confirm these findings, we used an ELISA-based Runx2 transcription factor assay, and the results revealed that the interaction between Runx2 and its target sequence sequences was significantly inhibited by EMD. We also reported here that EMD impaired activity of Runx2 in ECs. Numerous

evidence supports that VEGF is one of the target genes of Runx2, and VEGF-VEGFRs signaling is controlled by Runx2 activity (18,19,35). However, the direct evidence of the relationship between Runx2 and VEGFR-2 is still lacking. Therefore, on-going research is directed to exact the mechanisms of EMD on Runx2 and VEGFR-2 to clarify their causal relation.

In conclusion, we report that EMD, an anthraquinone derivative, impaired the metastatic and angiogenic potential of breast cancer, and the inhibitory effects were due to its ability to reduce the expression of MMP-9 and MMP-13 in breast cancer cells and the activation of VEGFR-2 in ECs. These effects may be associated with inhibition of transcriptional activity of Runx2.

Acknowledgements

This study was supported by grants from the National Natural Science Foundation of China (grant no. 81160530 and 81260656), National Basic Research Program of China ('973' Program) (grant no. 2010CB530603), Key Research Project from the Ministry of Education of China (grant no. 211091), and the Natural Science Foundation of Jiangxi Province (grant no. 2010GQY0147).

References

- Siegel R, Naishadham D and Jemal A: Cancer Statistics, 2013. *CA Cancer J Clin* 63: 11-30, 2013.
- Weigelt B, Peterse JL and van 't Veer LJ: Breast cancer metastasis: markers and models. *Nat Rev Cancer* 5: 591-602, 2005.
- Leong SP, Cady B, Jablons DM, *et al*: Clinical patterns of metastasis. *Cancer Metastasis Rev* 25: 221-232, 2006.
- Stevanovic A, Lee P and Wilcken N: Metastatic breast cancer. *Aust Fam Physician* 35: 309-312, 2006.
- Liu S, Goldstein RH, Scepansky EM, *et al*: Inhibition of rho-associated kinase signaling prevents breast cancer metastasis to human bone. *Cancer Res* 69: 8742-8751, 2009.
- Chiang AC and Massagué J: Molecular basis of metastasis. *N Engl J Med* 359: 2814-2823, 2008.
- Gupta GP and Massagué J: Cancer metastasis: building a framework. *Cell* 127: 679-695, 2006.
- Adams RH and Alitalo K: Molecular regulation of angiogenesis and lymphangiogenesis. *Nat Rev Mol Cell Biol* 8: 464-478, 2007.
- Duffy MJ, Maguire TM, Hill A, *et al*: Metalloproteinases: role in breast carcinogenesis, invasion and metastasis. *Breast Cancer Res* 2: 252-257, 2000.
- Roy R, Yang J and Moses MA: Matrix metalloproteinases as novel biomarkers and potential therapeutic targets in human cancer. *J Clin Oncol* 27: 5287-5297, 2009.
- Radisky ES and Radisky DC: Matrix metalloproteinase-induced epithelial-mesenchymal transition in breast cancer. *J Mammary Gland Biol Neoplasia* 15: 201-212, 2010.
- Lian JB, Stein JL, Stein GS, *et al*: Runx2/Cbfa1 functions: diverse regulation of gene transcription by chromatin remodeling and co-regulatory protein interactions. *Connect Tissue Res* 44 (Suppl 1): S141-S148, 2003.
- Karsenty G: Role of Cbfa1 in osteoblast differentiation and function. *Semin Cell Dev Biol* 11: 343-346, 2000.
- Komori T: Runx2, a multifunctional transcription factor in skeletal development. *J Cell Biochem* 87: 1-8, 2002.
- Stein GS, Lian JB, van Wijnen AJ, *et al*: Runx2 control of organization, assembly and activity of the regulatory machinery for skeletal gene expression. *Oncogene* 23: 4315-4329, 2004.
- Harada S and Rodan GA: Control of osteoblast function and regulation of bone mass. *Nature* 423: 349-355, 2003.
- Shore P: A role for Runx2 in normal mammary gland and breast cancer bone metastasis. *J Cell Biochem* 96: 484-489, 2005.
- Sun L, Vitolo MI, Qiao M, *et al*: Regulation of TGFbeta1-mediated growth inhibition and apoptosis by RUNX2 isoforms in endothelial cells. *Oncogene* 23: 4722-4734, 2004.
- Qiao M, Shapiro P, Fosbrink M, *et al*: Cell cycle-dependent phosphorylation of the RUNX2 transcription factor by cdc2 regulates endothelial cell proliferation. *J Biol Chem* 281: 7118-7128, 2006.
- Sun L, Vitolo MI and Passaniti A: Runt-related gene 2 in endothelial cells: inducible expression and specific regulation of cell migration and invasion. *Cancer Res* 61: 4994-5001, 2001.
- Liu A, Chen H, Wei W, *et al*: Antiproliferative and antimetastatic effects of emodin on human pancreatic cancer. *Oncol Rep* 26: 81-89, 2011.
- Kaneshiro T, Morioka T, Inamine M, *et al*: Anthraquinone derivative emodin inhibits tumor-associated angiogenesis through inhibition of extracellular signal-regulated kinase 1/2 phosphorylation. *Eur J Pharmacol* 553: 46-53, 2006.
- Fu J, Ding Y, Huang D, *et al*: The retinoid X receptor-selective ligand, LGD1069, inhibits tumor-induced angiogenesis via suppression of VEGF in human non-small cell lung cancer. *Cancer Lett* 248: 153-163, 2007.
- Hsu S-C and Chung J-G: Anticancer potential of emodin. *BioMedicine* 2: 108-116, 2012.
- Lu HF, Lai KC, Hsu SC, *et al*: Involvement of matrix metalloproteinases on the inhibition of cells invasion and migration by emodin in human neuroblastoma SH-SY5Y cells. *Neurochem Res* 34: 1575-1583, 2009.
- Chambers AF and Matrisian LM: Changing views of the role of matrix metalloproteinases in metastasis. *J Natl Cancer Inst* 89: 1260-1270, 1997.
- Fidler IJ: Angiogenesis and cancer metastasis. *Cancer J* 6 (Suppl 2): S134-S141, 2000.
- Inman CK, Li N and Shore P: Oct-1 counteracts autoinhibition of Runx2 DNA binding to form a novel Runx2/Oct-1 complex on the promoter of the mammary gland-specific gene beta-casein. *Mol Cell Biol* 25: 3182-3193, 2005.
- Barnes GL, Javed A, Waller SM, *et al*: Osteoblast-related transcription factors Runx2 (Cbfa1/AM13) and MSX2 mediate the expression of bone sialoprotein in human metastatic breast cancer cells. *Cancer Res* 63: 2631-2637, 2003.
- Inman CK and Shore P: The osteoblast transcription factor Runx2 is expressed in mammary epithelial cells and mediates osteopontin expression. *J Biol Chem* 278: 48684-48689, 2003.
- Jiménez MJ, Balbín M, López JM, *et al*: Collagenase 3 is a target of Cbfa1, a transcription factor of the runt gene family involved in bone formation. *Mol Cell Biol* 19: 4431-4442, 1999.
- Selvamurugan N and Partridge NC: Constitutive expression and regulation of collagenase-3 in human breast cancer cells. *Mol Cell Biol Res Commun* 3: 218-223, 2000.
- Selvamurugan N, Kwok S and Partridge NC: Smad3 interacts with JunB and Cbfa1/Runx2 for transforming growth factor-beta1-stimulated collagenase-3 expression in human breast cancer cells. *J Biol Chem* 279: 27764-27773, 2004.
- Pratap J, Javed A, Languino LR, *et al*: The Runx2 osteogenic transcription factor regulates matrix metalloproteinase 9 in bone metastatic cancer cells and controls cell invasion. *Mol Cell Biol* 25: 8581-8591, 2005.
- Kwon TG, Zhao X, Yang Q, *et al*: Physical and functional interactions between Runx2 and HIF-1 α induce vascular endothelial growth factor gene expression. *J Cell Biochem* 112: 3582-3593, 2011.